Journal of Applied Mechanics and Technical Physics, Vol. 44, No. 6, pp. 803–808, 2003

EFFECT OF WETTABILITY ON THE BEHAVIOR OF A LIQUID DROP AFTER ITS COLLISION WITH A SOLID SUBSTRATE

V. T. Borisov,[1] A. N. Cherepanov,[2] M. R. Predtechenskii,[3] and Yu. D. Varlamov[3]

UDC 532.501.32:535.347:535.52

A mathematical model is developed for the behavior of a small-diameter liquid drop after its collision with a solid surface, where the action of viscous forces can be neglected. The model takes into account the effect of adhesion interaction between the liquid and the substrate. Depending on the Weber number and equilibrium limiting wetting angle, it is shown that three regimes of drop motion are possible: adhesion without rebound, adhesion after rebound, and separation at the end of rebound. Regions of existence of these regimes are determined.

Key words: *drop, substrate, collision, adhesion, limiting wetting angle, mathematical model.*

Introduction. A collision of a liquid drop with a solid surface was considered in many papers in studying erosion of blades of hydraulic and steam turbines, blades of helicopter propellers, shields of antennas of aircraft radars, etc. [1–3]. Further development of investigations in this direction is associated with studying the processes of formation of powder coatings [4–6], deposition of ink microdroplets during of jet printing [7], and the behavior of small particles of solder injected onto a solid substrate (this process is used for assembling elements in microelectronics [8–14]).

In known mathematical models [8–14] proposed for the description of drop spreading on a substrate, the adhesion interaction of the liquid with the surface is taken into account rather approximately; therefore, the solutions obtained do not provide a detailed description of flattening, rebound, and recoil of particles from the substrate surface with limited wettability.

Based on the laws of conservation of mass and energy, a mathematical description of the behavior of a liquid drop after its incidence onto a solid surface is suggested in the present work. In contrast to the known model [4], it is assumed that the particle has a spherical shape at the moment of collision. In addition, the effect of capillary and adhesion effects is taken into account, which offers an adequate description of the processes of particle spreading and rebound and also the conditions of particle separation from the substrate.

Mathematical Model of the Process. Let a liquid drop of radius H_0 be incident onto a solid substrate perpendicular to the surface. The liquid is incompressible, and there is no heat exchange with the ambient medium and the substrate. It is also assumed that the shape of the flattening drop (Fig. 1a) is symmetric about the z axis and, at the time t, can be presented in the form of a spheroidal segment HM_2hH and a toroidal disk hM_2M_1ROh with a lateral semicircumference RM_1M_2R whose diameter is h. Note, in contrast to the model [4], the suggested shape of the drop is more adequate to the experimentally observed morphology of the particle at the initial stage of spreading [9, 11].

The velocity field inside the particle is set as follows: the velocity is identical everywhere inside the segment and is characterized only by the vertical component $v = v(t)$, the velocity inside the disk is characterized only by

[1]Central Research Institute of Ferrous Metallurgy, Moscow 107005. [2]Institute of Theoretical and Applied Mechanics, Siberian Division, Russian Academy of Sciences, Novosibirsk 630090. [3]Kutateladze Institute of Thermophysics, Siberian Division, Russian Academy of Sciences, Novosibirsk 630090. Translated from Prikladnaya Mekhanika i Tekhnicheskaya Fizika, Vol. 44, No. 6, pp. 64–69, November–December, 2003. Original article submitted September 4, 2002; revision submitted March 24, 2003.

0021-8944/03/4406-0803 $25.00 © 2003 Plenum Publishing Corporation

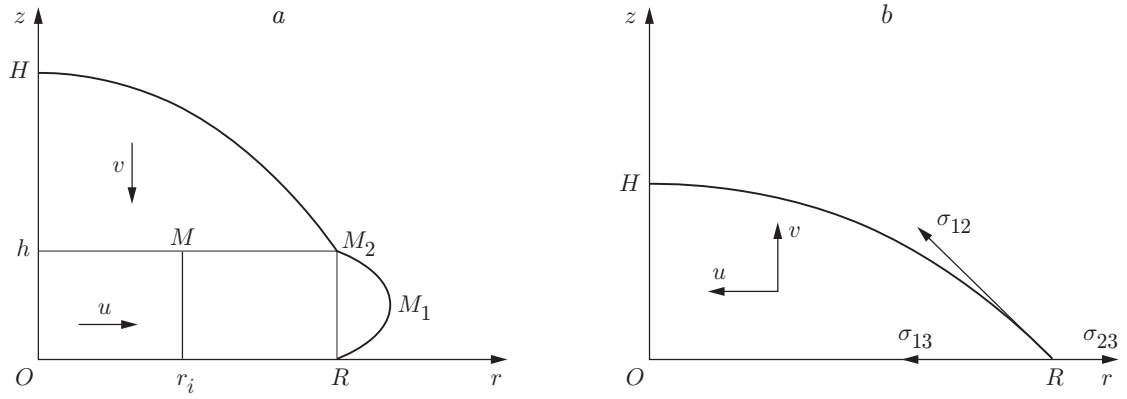

Fig. 1. Calculated shape of the drop during spreading (surge) (a) and during rebound (b).

the radial component $u(r,t)$, where

$$u = -\frac{r}{2h}\,v(t), \qquad 0 \leqslant r \leqslant R,$$
$$u = -\frac{R^2}{2hr}\,v(t), \qquad R \leqslant r \leqslant R + \frac{h}{2} \tag{1}$$

(R is the radius of the contact spot on the substrate).

The first expression in (1) is obtained under the condition that, for an arbitrary r_i, the flux of the substance through the surface Mr_i whose area is $2\pi r_i h$ ($0 \leqslant r_i \leqslant R$) is equal to the flux through the surface hM whose area is πr_i^2 (Fig. 1a). The second expression follows from the solution of the continuity equation for an incompressible liquid under the condition that the first equality in (1) is satisfied at the boundary $r = R$. In this case, we have $v(t) = \dot{H}(t)$ [$H(t)$ is the total height of the particle; the dot indicates the derivative with respect to t].

To calculate the energy quantities, we first determine the expressions for the geometric characteristics of the corresponding elements of the deformed particle (Fig. 1a). The volume Ω_1 and surface S_1 of its spheroidal part are described by the relations

$$\Omega_1 = \pi(H-h)((H-h)^2 + 3R^2)/6, \qquad S_1 = \pi((H-h)^2 + R^2), \tag{2}$$

and those for the toroidal part, by the relations

$$\Omega_2 = \pi h(R^2 + \pi Rh/4 + h^2/6), \qquad S_2 = \pi h(\pi R + h). \tag{3}$$

It is also assumed that the parameters h and H are related as

$$h = H(1 - H/H_0)^n, \tag{4}$$

where H_0 is the initial drop diameter and n is a constant chosen for best fitting to the experiment. From the condition of a constant volume of the drop $\Omega_1 + \Omega_2 = \pi H_0^3/6$, where the expressions for Ω_1 and Ω_2 follow from (2) and (3), we obtain the dependence $R(H)$ in the form

$$R = h\sqrt{Y^2 - \frac{H^3 - H_0^3}{3h^2(H+h)} + \frac{H}{h}\,\frac{H-h}{H+h}} - Y,$$

where $Y = (\pi/4)[h/(H+h)]$; the value of h is determined by formula (4).

The potential energy of the drop–substrate system is found from the relation

$$P = (S_1 + S_2)\sigma_{12} + \pi R^2(\sigma_{13} - \sigma_{23}) - \pi H_0^2\sigma_{12},$$

where σ_{12}, σ_{13}, and σ_{23} are the surface tensions on the liquid–gas, liquid–substrate, and substrate–gas interfaces, respectively. Here, the potential energy of the initial state $P_0 = \pi H_0^2\sigma_{12}$ corresponding to the moment when the drop touches the substrate is used as a reference point. We determine the total kinetic energy of the drop K by integrating its elementary values over each of the above-mentioned volumes Ω_i: $K = \dfrac{\rho}{2}\sum\limits_i \int v_i^2\, d\Omega_i$, where ρ is the density of the liquid.

We pass to dimensionless quantities, using H_0, v_0, and $K_0 = \pi H_0^3 \rho v_0^2/12$ for scaling. After appropriate transformations, we obtain the following expressions for the dimensionless functions $\bar{K} = K/K_0$ and $\bar{P} = P/K_0$:

$$\bar{K} = v^2(1 - h^3 F(z)), \qquad \bar{P} = 12[(\bar{H} - \bar{h})^2 + \bar{h}^2(G(z) - z^2\cos\theta) - 1]/\,\mathrm{We}\,. \tag{5}$$

Here $H = H/H_0$, $z = R/h$, $\bar{h} = h/H_0$, $\bar{v} = v/v_0$, v_0 is the velocity of collision between the drop and the substrate, θ is the equilibrium limiting wetting angle, We is the Weber number, $G(z) = 1 + \pi z + z^2$, and $F(z) = G(z) - 3z^4 I(z)$, where

$$I(z) = \begin{cases} (4z^2-1)^{1/2} \arctan\sqrt{\dfrac{2z-1}{2z+2}} - 1 + \pi z, & 2z \geqslant 1, \\ (1-4z^2)^{1/2} \ln\left|\dfrac{\sqrt{1-2z}+\sqrt{1+2z}}{\sqrt{1-2z}-\sqrt{1+2z}}\right| - 1 + \pi z, & 2z \leqslant 1. \end{cases} \tag{6}$$

In the case of drop spreading (surge), an increase in surface energy of the drop, release of heat Q due to the work performed by adhesion forces $[A = 2\pi R^2 \sigma_{12}(1 + \cos\theta)]$, and dissipation of this heat (except for the case $\cos\theta = -1$, where $A = 0$) are observed. The law of energy conservation in this period has the form

$$\bar{K} + \bar{P} + \bar{Q} = 1. \tag{7}$$

In what follows, the bar over the dimensionless quantities is omitted. Since the rate of drop spreading during surge is significantly higher than the rate of natural spreading of the drop over the substrate under the action of molecular forces, the greater part of work of adhesion in the surge stage is converted into heat. Therefore, assuming that $\bar{Q} = \bar{A}$, where

$$\bar{A} = 12\bar{R}^2(1 + \cos\theta)/\,\mathrm{We}, \tag{8}$$

and substituting expressions (5), (6), and (8) into (7), after appropriate transformations, we obtain the differential equation that describes the surge stage:

$$(1 - h^3 F(z))\dot{H} = 1 - 12((H - h)^2 + h^2 G(z) + R^2 - 1)/\,\mathrm{We}, \qquad R = zh.$$

Here we take into account that $v = \dot{H}$; the dot indicates the derivative with respect to the parameter $\tau = tv_0/H_0$. To solve this equation, we use Eqs. (3) and (4) and the initial condition $H(0) = 1$. The equation is valid until the maximum spreading of the drop reached at the time $\tau = \tau_*$ determined by the equality $K(\tau_*) = 0$.

Thus, the kinetics of the considered spreading process depends only on the Weber number We. In particular, the parameters of the maximum spreading (time τ_*, contact-spot radius R_*, and height H_*) depend only on the Weber number; the quantity R_* is satisfactorily approximated by the formula

$$R_* = \sqrt{(w - 1/w^2)/3}, \qquad w = 1 + 0.15\,\mathrm{We}\,. \tag{9}$$

In the process of the reverse motion of the drop (rebound), the natural shape is a spherical segment (Fig. 1b) acquired by the drop after spreading is finished. This process of transformation of the shape shown in Fig. 1a to the shape shown in Fig. 1b is caused by the tendency to equalization of the Laplace pressure and minimization of the surface area of the drop and, apparently, occurs so rapidly that the time needed for this transformation can be ignored. The shape is changed with a constant radius of the contact spot R_* and an unchanged volume of the drop. As a result, the new height of the drop H_{**} is determined by the equation

$$H_{**}(H_{**}^2 + 3R_*^2) = 1. \tag{10}$$

In transformation, some part of the potential energy of the drop dissipates because of the decrease in its surface area. After transformation, the potential energy can be determined as

$$P_{**} = 12(H_{**}^2 + R_*^2(1 - \cos\theta) - 1)/\,\mathrm{We}\,. \tag{11}$$

The distribution of velocity components of the liquid flow inside the segment at the stage of rebound is accepted in the form

$$v = z\dot{H}/H, \qquad u = -r\dot{H}/(2H), \tag{12}$$

which ensures satisfaction of the continuity equation. The kinetic energy is calculated by integrating the kinetic energy density equal to $\rho(v^2 + u^2)/2$ over the segment volume. The potential energy is determined by the expression

$$P = 12(H^2 + R^2(1 - \cos\theta) - 1)/\,\mathrm{We}\,. \tag{13}$$

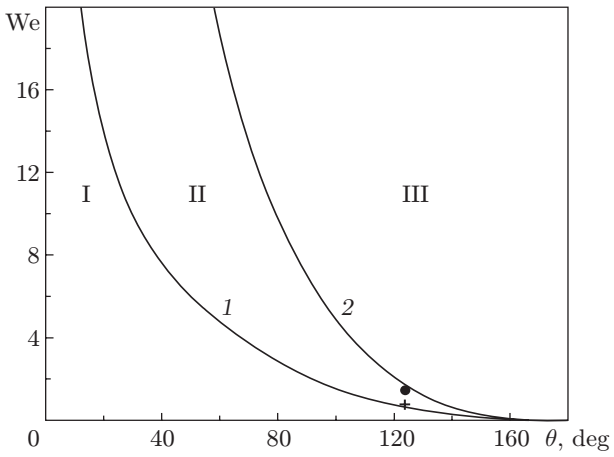

Fig. 2

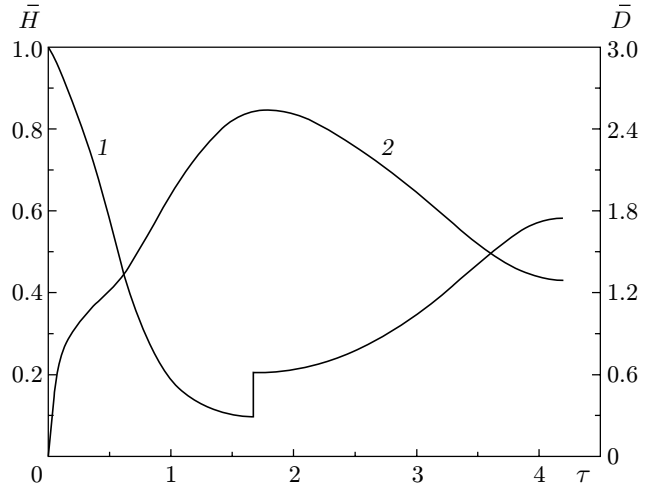

Fig. 3

Fig. 2. Regions of drop motion on the substrate: adhesion without rebound (I), adhesion after rebound (II), and separation after rebound (III); curves 1 and 2 refer to the "quiescent" state and separation; the points are the experimental data of [11].

Fig. 3. Variation of the relative height $\bar{H}$ (1) and contact-spot diameter $\bar{D}$ (2) during drop spreading and rebound with subsequent adhesion to the substrate for We = 15 and $\theta = 45^\circ$.

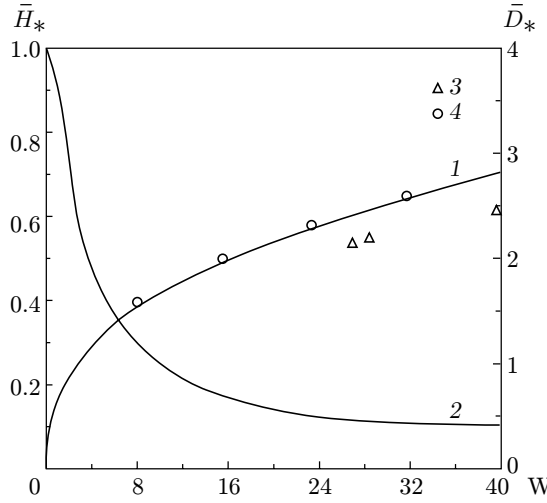

Fig. 4. Relative values of the contact-spot diameter (1, 3, and 4) and liquid-drop height (2) versus the Weber number: curves 1 and 2 refer to numerical calculations, points 3 are the experimental data of [13], and points 4 show the calculation by formula (9).

The work of separation of the drop from the substrate, equal to the work of adhesion, is performed due to energy of the drop; therefore, the law of energy conservation has the form

$$K + P = P_{**}. \tag{14}$$

Integrating the kinetic energy density over the segment volume with allowance for (12) and substituting the resultant expression and relation (13) into (14), we obtain the differential equation that describes the rebound stage:

$$\dot{H}^2\varphi(H) + 12(H^2 + R^2(1 - \cos\theta) - 1)/\,\mathrm{We} = P_{**}. \tag{15}$$

Here $\varphi(H) = (13/90)H^3 + 11/36 + (1/36)H^{-3}$ and the value of P_{**} is determined by Eqs. (10) and (11). Equation (15) is solved under the initial condition $H(0) = H_{**}$.

Analysis of Results. The results of numerical investigations showed that the behavior of the drop on the substrate after the maximum spreading of the liquid depends significantly on the Weber number and equilibrium limiting wetting angle θ. Three regimes of drop motion are possible: adhesion without rebound, adhesion after rebound, and separation at the end of rebound. The existence regions for these regimes are determined (Fig. 2). For values of We and θ corresponding to curve 1 ("quiescent" curve), the drop after the maximum spreading acquires a thermodynamically equilibrium shape. The angle at the drop base after transformation equals the equilibrium limiting wetting angle, and no rebound is observed after spreading. Below this curve, there is no rebound either, but the angle at the base of the transformed drop differs from the equilibrium value. Above curve 1, at a small distance from it, rebound occurs with a low velocity. The latter increases with approaching of the figurative point (We, θ) to curve 2 above which there occurs drop separation from the substrate with a velocity increasing with distance from this curve. Rebound with subsequent adhesion is observed if the point (We, θ) is located between curves 1 and 2.

It was experimentally found in [12] that, for We = 0.7, a mercury drop colliding with a glass substrate ($\theta = 123^\circ$) moves backward after spreading with subsequent adhesion; for We = 1.2, it recoils from the substrate at the end of rebound. These values of We and θ correspond to the points in Fig. 2. They are located close to boundaries 1 and 2 of the corresponding regions.

Figure 3 shows the dynamics of the behavior of the drop on the substrate. When complete spreading is reached at the time $\tau = 1.64$, the drop shape changes rapidly; after that, at given values We = 15 and $\theta = 45^\circ$, the rebound stage occurs, which is completed by drop adhesion to the substrate.

The solid curves in Fig. 4 show the calculated dependences of the drop spreading parameters on the Weber number. Points 3 refer to the experimental data on the diameter of the maximum spreading of drops of water and water solutions of sodium carbonate over a steel substrate for various Weber numbers [13], and points 4 are the results of calculations by the approximate formula (9). The greater calculated values of the contact-spot diameter during the maximum spreading are, probably, caused by the neglect of viscosity of the liquid medium in the mathematical model. Taking into account the experimental errors and the assumptions used in constructing the mathematical model, we believe that the agreement of numerical and experimental results can be considered as satisfactory.

The model proposed can be used to rapidly evaluate the parameters of the process under consideration, since the calculation time of one variant on IBM-482 is about 1 min.

REFERENCES

1. G. F. Schmitt (Jr.), "Current investigation in rain erosion by the U.S. air force," Preprint, New York, S. n. (1966).
2. A. A. Fyall, R. B. King, and R. N. C. Strain, "Rain erosion aspects of aircraft and guided missiles," *J. Roy. Aeronaft. Soc.*, **66**, 447–453 (1962).
3. G. S.Springer, *Erosion by Liquid Impact*, John Wiley and Sons, New York (1976).
4. J. Madejski, "Solidification of droplets on a cold surface," *Int. J. Heat Mass Transfer*, **19**, 1009–1013 (1976).
5. D. A. Gasin and B. A. Uryukov, "Dynamics of interaction of a liquid drop with a surface," *Izv. Sib. Otd. Akad. Nauk SSSR, Ser. Tekh. Nauk*, Issue 2, No. 16, 95–100 (1986).
6. M. F. Zhukov and O. P. Solonenko, *High-Temperature Dusty Jets in Processing Powder Materials* [in Russian], Inst. Thermophysics, Sib. Div., Acad. of Sci. of the USSR, Novosibirsk (1990).
7. A. Asai, S. Makoto, S. Hirasawa, and T. Okasaki, "Impact of an the drop on paper," *J. Image Sci. Technol.*, **37**, 205 (1993).

8. Z. Zhao, D. Poulikakos, and J. Fukai, "Heat transfer and fluid mechanics during the collision a liquid droplet on a substrate. 1. Modeling," *Int. J. Heat Mass Transfer*, **39**, 2771–2789 (1996).
9. J. M. Waldvogel and D. Poulikakos, "Solidification phenomene in picoliter sire solder droplet deposition on a composite substrate," *Int. J. Heat Mass Transfer*, **40**, 295–309 (1997).
10. B. Xiong, C. M. Megaridis, D. Poulikakos, et al., "An investigation of key factors affecting solder microdroplet deposition," *J. Heat Transfer*, **120**, 259–269 (1998).
11. M. R. Predtechenski, A. N. Cherepanov, V. N. Popov, and Yu. D. Varlamov, "Crystallization dynamics of a liquid metal drop impinging onto a multilayered substrate," *J. Appl. Mech. Tech. Phys.*, **43**, No. 1, 93–102 (2002).
12. S. Schiafino and A. A. Sonin, "Molten droplet deposition and solidification at low Weber number," *Phys. Fluids*, **9**, No. 11, 3172–3187 (1997).
13. M. Pasandideh-Fard, J. M. Qiao, S. Chandra, et al., "Capillary effects during droplet impact on a solid surface," *Phys. Fluids*, **8**, No. 3, 650–659 (1996).
14. J. Fukai, Y. Shiiba, T. Yamamoto, et al., "Wetting effects on the spreading of a liquid droplet cooling with a flecs surface: Experiment and modelling," *Phys. Fluids*, **7**, No. 2, 236–247 (1995).